Nanosecond photolytic interruption of bacteriorhodopsin photocycle

K-590 → BR-570 reaction

V. Bazhenov, P. Schmidt, and G. H. Atkinson
Department of Chemistry and Optical Science Center, University of Arizona, Tucson, Arizona 85721 USA

ABSTRACT The molecular processes comprising the room temperature bacteriorhodopsin (BR) photocycle are examined through the properties of the photo-induced reverse reaction, K-590 + hν → BR-570 (K → BR). Two sequential pumping pulses, each of 10-ns duration, are used, respectively, to initiate the photocycle via the forward BR-570 + hν → K-590 (BR → K) reaction (532 nm) and to photolytically interrupt the thermal BR photocycle after a 20-ns delay via K → BR (620–700 nm). The ground-state BR-570 population, monitored by 633-nm absorption 200 μs after the photocycle begins, provides a quantitative measure of the efficiency with which K → BR interrupts the photocycle to reform BR-570. The quantum yield (Φ) for K → BR is found to be 1.6 ± 0.1 times larger than that for BR → K which, when compared to a Φ of 0.64 for BR → K, suggests that Φ for K → BR is ≈ 1.0. The significance of such a high efficiency K → BR reaction with respect to mechanistic descriptions of the BR photocycle is discussed.

INTRODUCTION

The photochemical reactions of bacteriorhodopsin (BR), the trans-membrane protein in *Halobacterium halobium,* have been examined extensively for a variety of reasons. Many studies have sought to elucidate the molecular processes that underlie its biochemical function in bacteria, while others have focused on relationships between the BR photocycle and the rhodopsin photochemistry involved in vision (1–3). Recently, films of BR have been shown to have optical properties (e.g., photochromism, light-induced dichroism, and birefringence) that can be used for fast optical processing and holography extending over a wide time range (10^{-12} to 10^{3} s) (4, 5).

The molecular and spectroscopic properties of the BR photocycle are of central interest in all of these studies (2, 3). The BR photocycle encompasses a series of consecutive reactions involving specific isomeric and conformational forms of the retinal chromophore and the corresponding protein environments that, together, efficiently transform absorbed light into chemical energy (2, 3). With optical pumping of <5 ps duration, primarily one excited electronic state (BR*, lifetime of 500 fs) is populated (6). The remainder of the photocycle proceeds on ground-state potential surfaces (i.e., thermally) (2) and is comprised of at least six intermediates: BR-570 + hν → BR* → J-625 → K-590 → L-550 → M-412 → N-550 → O-610 → BR-570, where the numbers indicate wavelengths (nm) of absorption maxima (2, 7). The presence of other intermediates, including a KL species formed between K-590 and L-550 (8–10), and more than one photocycle each with its own intermediates connected by a specific kinetic mechanism has been suggested (11, 12), but in this work the photocycle presented above is used.

The mechanism(s) involving the primary BR photocycle intermediates (J-625 and K-590) is of particular interest because their properties appear to be representative of many molecular systems that control light energy transformation in living organisms (3). The storage of the ≈ 11.6 kcal/mol of energy needed to drive the trans-membrane proton pumping in BR, and thereby ATP synthesis in the bacterium, is associated particularly with K-590 (13). Since the absorption spectra of BR-570 and K-590 are strongly overlapped and since an optically-induced back reaction, K-590 + hν → BR-570 (denoted here as K → BR), occurs with high efficiency (14, 15), optical excitation of the BR photocycle is complicated by the formation of photo-stationary mixtures of several species (e.g., BR-570, J-625, K-590, and their associated excited electronic states).

The forward reaction mechanism at room temperature has been studied extensively, but the reverse reaction(s) by which light can interrupt the 20-ms thermal photocycle to reform BR-570 has been studied only under special experimental conditions. Low temperature (77K), solid BR samples have been examined because at least one intermediate can be thermally stabilized (16–22). For example at ≈ 10K, where K-590 is thought to be trapped, the efficiency of K → BR conversion is reported to be ≈ 100% when excitation

V. Bazhenov's permanent address is Institute of Physics, Academy of Sciences Ukrainian SSR, Prospect Nauki, 46, Kiev 252650, USSR.
Address correspondence to G. H. Atkinson.

0006-3495/92/06/1630/08 $2.00

wavelengths > 650 nm are used (17) (quantum yield, Φ, of 0.7 [18, 19]). The K → BR conversion occurs in < 30 ps at both 13K (21) and 6.5K (22). Delays of a few seconds between the optical initiation of the forward and reverse reactions do not critically affect the 10K results because K-590 is considered stable at this temperature. Since the protein is also frozen in these samples, it is not clear how low temperature results relate to the room temperature photocycle. The K → BR reaction also has been studied previously in room temperature BR samples (14, 15), but only with high pump energies that create a photostationary mixture of BR-570 and photocycle intermediates. The photostationary mixture created by single-pulsed excitation permits the kinetic analysis to be simplified (14, 15), but does not provide the experimental opportunity to independently investigate the dependence of the K → BR efficiency on either the power or wavelength of the laser radiation used to excite K-590. These studies have determined $\Phi_{K\rightarrow BR}/\Phi_{BR\rightarrow K}$ for a specific photostationary mixture (14, 15).

The photoinduced M → BR reaction also has been examined at room temperature with time-resolved (10 ns) resonance Raman spectroscopy (23). With 10-ns excitation, the M → BR reaction is accessible both spectroscopically (absorption spectra of BR-570 and M-412 are well separated) and temporally (J → K in < 10 ps, K → L in ≈ 2 μs, and M → BR in ≈ 20 ms [2]). The M-412 intermediate, therefore, can be experimentally observed independent of the other photocycle intermediates even though 10-ns excitation creates a photostationary distribution of species (2). In this respect, the M → BR and K → BR reactions are significantly different because the BR-570 and K-590 absorption spectra are strongly overlapped, making it difficult to extract kinetic information from single-laser data (24, 25). In general, therefore, the molecular dynamics of the room temperature K → BR reaction are neither well understood or quantitatively modelled.

The biophysical importance of elucidating the primary photocycle events (both forward and reverse reactions) in room temperature BR has been widely discussed (1–3). A similar interest exists for optical processing applications of BR films where room temperature operation would be advantageous. The efficiencies of the BR → K and K → BR reactions are especially important because both photostability and high contrast "read" mechanisms may rely on quantitatively controlling the relative concentrations of the initial intermediates. Given the available understanding of BR → K, it is evident that the K → BR reaction needs to be examined in more detail at room temperature where data can be related directly to the biophysical membrane and to the experimental conditions sought for optical processing.

In this paper, the photoinduced K → BR reaction is investigated at room temperature with a double-pump experimental configuration using two pulsed (10 ns) dye lasers. Tunable radiation in the 620–700 nm region, delayed 20 ns after the photocycle is initiated by 532-nm excitation, is used to optically interrupt the BR photocycle by reforming BR-570 from K-590. The relative amount of ground-state BR-570 is measured subsequentially at a 200-μs delay (after 532 nm excitation) by the absorbance at 633 nm. The double-pump experiments permit the power and wavelength dependencies underlying the K → BR reaction together with the overall conversion efficiency to be studied throughout the 620–700-nm region. The properties of the excited electronic state of K-590 (K*), the protein environment(s) that facilitate the reformation of BR-570, and the significance of the relative efficiencies of the BR → K and K → BR reactions are discussed.

EXPERIMENTAL

Materials and instrumentation

The BR purple membrane is prepared using published procedures (26) from strain R-1 and is examined as a sample in a water suspension (pH 6.6) placed in a 1-mm thick quartz cell (sample OD = 0.62 at 570 nm).

The laser instrumentation (Fig. 1) is comprised of a pulsed Q-switched Nd:YAG laser (Quanta-Ray DCR-2) and a dye laser (Quanta Ray PDL-1). The 100 mJ frequency doubled output from the Nd:YAG (10-ns pulse) is used to pump the dye laser (oscillator and amplifier) operating with either a DCM or LDS698 dye mixture. The dye laser outputs cover the 610–740-nm spectral range with maximum pulse energies of 20 mJ. Approximately 7.5 mJ/cm² of the 532 nm output (measured at sample after passing PR_2 and P; Fig. 1) is used to

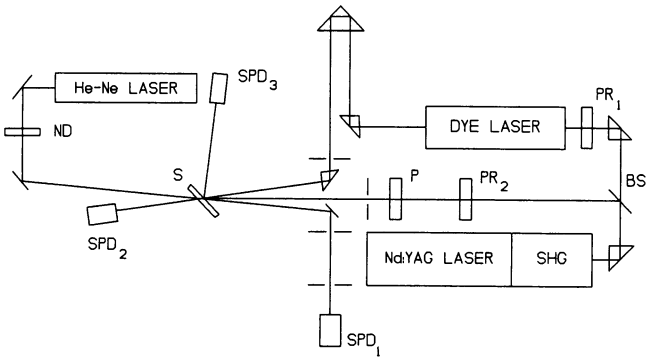

FIGURE 1 Schematic representation of experimental instrumentation. The excitation pulses are produced by either the Nd:YAG laser (532 nm) or the dye laser (620–700 nm) which is pumped at 532 nm. Transient absorption measurements are made at 633 nm using a low energy He-Ne laser. Abbreviated symbols are: ND, neutral density filter; SPD, silicon photodiode; S, BR sample; P, polarizer; PR, polarization rotator; BS, beam splitter; SHG, second harmonic generating crystal for 1.06 μm to 532 nm.

initiate the BR photocycle and thereby to form K-590. The energy of the polarized pump radiation is varied by adjusting a polarization rotator (PR_2) located before the 532-nm beam reaches the sample (Fig. 1). Polarizer (P) serves to retain the same (vertical) polarization of the exciting radiation. The second excitation of the BR sample, which photolytically induces K → BR, occurs ≈ 20 ns after the 532-nm initiation of the photocycle and is achieved with the tunable dye laser output after it passes through an optical delay line. The pulse sequence used in these experiments together with the molecular mechanism describing the early stages of the BR photocycle are presented in Fig. 2.

The effectiveness of the optical interruption (K → BR) is determined by monitoring the amount of BR-570 through its 633-nm absorbance 200 μs into the photocycle (Fig. 2). A probe beam from a cw He-Ne laser (633 nm) measures the transient absorbance with an intensity of 0.5 mW/cm² which is reduced by a neutral density filter (ND; Fig. 1) to be itself nonperturbing with respect to the photocycle. All three laser beams have the same (vertical) polarization and are spatially overlapped within the plane of sample with beam cross-sections of: 4 mm² (532 nm), 1 mm² (dye laser), and 0.5 mm² (633 nm). The 633-nm intensity is monitored with a silicon photodiode biased with 90 V DC. Apertures are used to provide uniform illumination of the sample and to protect the diode from excessive scattered light. The photodiode output is amplified (Tektronix TM 503 with DC offset; Beaverton, OR) and read with an oscilloscope (Tektronix 475 A) operating with a 1-μs temporal resolution. All measurements are made with the Nd:YAG laser operating in a single pulse, Q-switched mode. The energy of each dye laser pulse is determined with a spectrally-nonselective energy meter (Scientech model 365; Boulder, CO).

The transient absorption spectrum of K-590 is measured with the dye laser radiation (delayed by 20 ns) as a probe. The intensity of this probe beam is reduced to a value that converts <3% of BR-570 into photocycle intermediates. For the measurement of spectra, two matched photodiodes are used: one (SPD_2) measuring the energy of the transmitted dye laser beam, and the second (SPD_3) measuring the energy of beam reflected from the first glass surface of the sample cell (reference value).

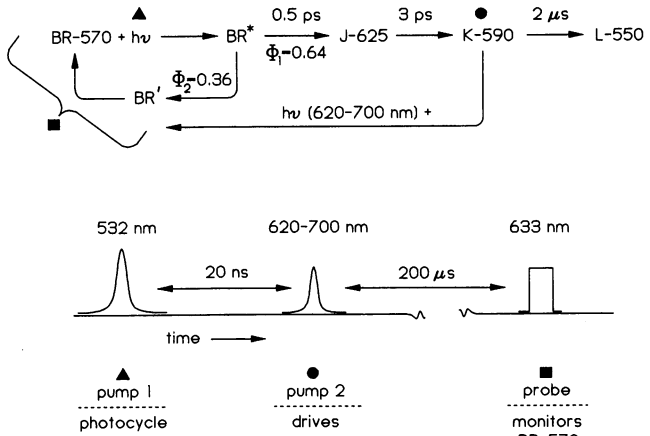

FIGURE 2 Laser pulse sequence for double excitation and 633 nm monitoring in the room temperature BR photocycle. The photocycle species involved in the initiation of the forward reaction and the photolytic interruption (K → BR) also are shown together with approximate rates and the quantum efficiencies involving BR*.

Procedure

The relative efficiencies of the BR → K and K → BR reactions are reflected in the percentage of BR-570 that is converted into photocycle intermediates after the sequential excitation at 532 nm and 620–700 nm (Fig. 2). Clearly, the transient concentrations of BR-570 and K-590 can be monitored to determine this value, but as long as the probe beam is photolytically nonperturbing, other photocycle intermediates also can be used. For example, transient absorption at 633 nm, monitors several different photocycle intermediates and/or populations depending on when, after excitation, the signal is measured (i.e., at increasingly longer delays: BR-570 (and vibrationally-excited BR, BR'), K-590, L-550, and O-610). Thus, different parts of the 633-nm transient absorption signal can be used to determine the percentage of BR-570 converted into photocycle intermediates. As in previous studies of the quantum efficiency of BR photochemistry (27–29), the 633-nm absorption signal at a 200-μs delay is used to monitor BR-570 because the other intermediates do not absorb significantly (<3%) under these conditions. The quantitative relationships between the relative efficiencies of BR → K and K → BR and the excitation conditions (i.e., powers of the two pump lasers) can be used to determine the relative efficiencies of the two reactions *vide infra*.

In the measurements presented here, the relative changes observed in the 633-nm transient absorption data are not affected (within ≈5%) by differences in the pumping conditions. This independence is found for both single pulse pumping (532-nm excitation only or 620–700-nm dye laser excitation only) and two-pulse sequential pumping with different pulse energies ratios (532-nm pulse followed at a 20-ns delay by 620–700-nm pulse). The kinetics observed are independent of the pumping used and, therefore, the 633-nm single (absorbance changes) at 200-μs delay remains proportional to the concentration of BR-570. A 200-μs time delay, monitoring the L-550 → M-412 reaction (Fig. 2), is selected in order to optimize the observed signal to noise ratio.

Since the absorption spectra of BR-570 and K-590 are strongly overlapped (2), the specific wavelength of nanosecond laser excitation strongly influences the photostationary mixture of the two species created. With the maximum of K-590 absorption shifted to the red by 20–30 nm relative to that of BR-570 (2), laser excitation in the green (<560 nm) is more effective in maximizing the concentration of K-590, while excitation in the red (>620 nm) is more effective for initiating the K → BR reaction. To determine the relative importance of the forward and reverse reactions underlying this photostationary mixture, data are obtained for a range of dye laser wavelengths (at 20 ns delay) both with and without 532-nm excitation. The energy density of the 532-nm pulse is chosen to be near the saturation value (0.3 mJ/mm²) and remains constant for these measurements.

It should be noted that with a 15 pulse/s laser repetition rate and a static sample, ≈ 10% of the BR-570 excited accumulates in a long lived (≈2 min) intermediate that has not been identified. To avoid accumulating this intermediate, a repetition rate of 2 pulses/min is used by reducing the *Q*-switching rate for the Nd:YAG laser while permitting the flashlamp pumping rate of the crystal to remain at 15 pulses/s (to ensure thermal stability and thereby maintaining good pulse energy reproducibility).

RESULTS AND DISCUSSION

Although the BR → K and K → BR reactions are known to dominate the early stages of the photocycle (Fig. 2), it

remains to be established whether other competing photolytically-induced reactions are present. This issue can be examined by measuring the 633-nm absorbance (A_{pr}) as a function of the dye laser (620–700 nm) pumping energy both with and without 532-nm pumping. The experimental results (Fig. 3) show that with only dye laser excitation in the red (e.g., 650 nm), 633-nm absorbance decreases until it becomes saturated in the region between 5 and 20 mJ/mm^2. This saturation reflects the concentration of photocycle intermediates reaching a maximum and corresponds to the conditions under which the largest percentage of BR-570 is converted into photocycle intermediates. By contrast, A_{pr} increases as the dye laser (650 nm) pulse energy increases when it follows 532-nm pumping by a 20-ns delay (Fig. 3). The two curves approach each other to within 5% when the red dye laser energy is $\approx$10–20 mJ/mm^2. Thus, >95% of the BR-570 excited to BR* decays to produced K-590 (i.e., via BR $\rightarrow$ K) and >95% of the K-590 excited to K* decays to reform BR-570 (i.e., via K $\rightarrow$ BR) *vide supra*. The 5% uncertainty represents the experimental error of the measurement, which is difficult to reduce because higher red dye laser energies result in the rapid degradation (i.e., irreversible bleaching) of the BR sample. These results demonstrate, therefore, that within 20 ns of optical initiation, high efficiency cycling between BR-570 and K-590 can be photoinduced. Qualitatively, this induced photocycling reflects the strongly overlapped absorption spectra of BR-570 and K-590, which ensures that both species undergo light-induced conversion to the other when either 532- or 620–700-nm excitation is used. The specific excitation conditions, therefore, significantly alter the concentrations of BR-570 and K-590.

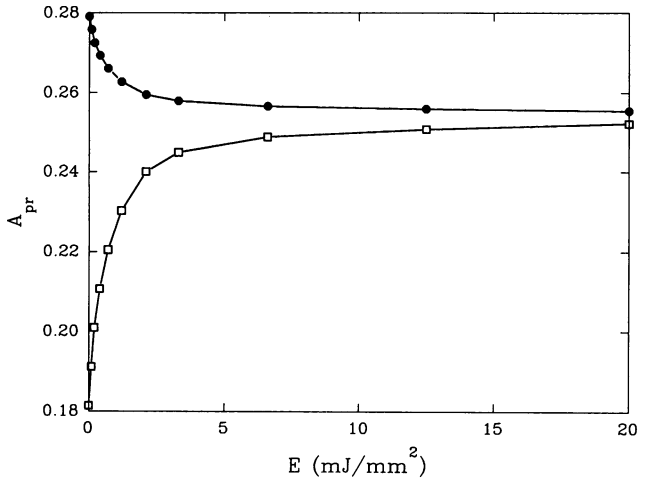

FIGURE 3 Dependence of 633 nm probe absorbance (A_{pr}) on the energy density of the pulsed (10 ns) 650-nm excitation. Data are recorded with (*open squares*) and without (*filled circles*) 532-nm pumping (see Fig. 2). The 650-nm dye laser beam is slightly focused to provide variable energy densities of up to 20 mJ/mm^2.

A quantitative analysis of BR $\rightarrow$ K and K $\rightarrow$ BR begins by considering only the photolytic effects of 620–700-nm excitation (the effect of 532-nm excitation appears as a constant). The concentrations of the two species after optical excitation are of primary interest in this part of the analysis. When $n_{BR}(t)$ and $n_K(t)$ denote the normalized concentrations of BR-570 and K-590, respectively, the light-induced changes are given by:

$$\frac{dn_{BR}(t)}{dt} = [-n_{BR}(t)\alpha_{BR} + n_K(t)\alpha_K]\frac{I(t)}{h\omega}$$
$$\frac{dn_K(t)}{dt} = [-n_K(t)\alpha_K + n_{BR}(t)\alpha_{BR}]\frac{I(t)}{h\omega}. \quad (1)$$

α_{BR} and α_K are the efficiencies ($=\sigma(\lambda)\Phi$, where σ is the absorption cross-section, Φ is the quantum yield for each photoinduced reaction, and the excitation intensity is $I(t)$). Since no other photoinduced reactions are present (*vide supra*),

$$n_{BR}(t) + n_K(t) = 1, \quad (2)$$

and only $n_K(t)$ needs to be considered:

$$\frac{dn_K(t)}{dt} = [-n_K(t)\alpha_K + [1 - n_K(t)]\alpha_{BR}]\frac{I(t)}{h\omega}. \quad (3)$$

Of specific interest is the value n_K, the concentration of K-590 following the photolytic pulse of energy density, E. An analytic solution to expression 3 is:

$$n_K = \frac{\alpha_{BR}}{(\alpha_{BR} + \alpha_K)} + \left[N_K - \frac{\alpha_{BR}}{(\alpha_{BR} + \alpha_K)}\right]e^{-E(\alpha_{BR}+\alpha_K)/h\omega}, \quad (4)$$

where the initial concentration of K-590 before the photolytic pulse is treated by introducing N_K. The value of n_K obtained from expression 4 represents that part of K-590 which is not optically converted back to BR-570, but which rather proceeds through the thermal photocycle.

Even when the energy density of the red pulse (620–700 nm) is not known, the ratio between α_{BR} and α_K can be calculated from expression 4 if two different N_K values are used. One N_K value (namely 0) can be obtained from the single laser data, but determination of a second value requires a double-pump laser experiment in which n_K ($= -\delta A_{pr}/A_{pr}$) is determined from changes in the 633-nm absorbance (δA_{pr}) measured 200 μs after excitation (Figs. 2 and 3). The value of n_K corresponds to the depletion of ground-state BR-570. n_K^0 represents the case $N_K = 0$. The results from the double-pulse experi-

ments are used to determine n_K. The N_K is given by $(A_{pr0} - A_{pr1})/A_{pr0}$, where the subscripts 0 and 1 denote, respectively, the absence and presence of 532-nm excitation. The N_K value found for the 532-nm excitation used here corresponds to 30–40% ground-state BR-570 depletion. Background absorption and scattering losses limit the accuracy with which the N_K value can be determined.

To minimize possible saturation effects, α_{BR} and α_K are evaluated in the limit of low energy (E) 620–700 nm excitation. Experimentally, the dye laser power is reduced until δA_{pr}, the change in absorbance, is $\approx 3\%$ of $(A_{pr0} - A_{pr1})$ caused by 532-nm excitation. Under these low energy conditions, it is feasible to describe the measured absorbance changes normalized to E:

$$D_{12} = \frac{A_{pr1} - A_{pr12}}{E(A_{pr1} - A_{pr0})} = \frac{N_K - n_K}{EN_K}$$

$$D_2 = \frac{A_{pr2} - A_{pr0}}{E(A_{pr1} - A_{pr0})} = \frac{n_K^0}{EN_K}. \quad (5)$$

The first expression in Eq. 5 is for two laser excitation (subscript 12 denotes 532- followed by 620–700-nm excitation) and the second is for one laser excitation (subscript 2 denotes 620–700-nm excitation only) (Fig. 4). The value of $(A_{pr1} - A_{pr0})$ is taken from 532-nm data.

Expression 4 is linearized to obtain:

$$n_K = N_K\left[1 - \frac{E(\alpha_{BR} + \alpha_K)}{h\omega}\right] + \frac{E\alpha_{BR}}{h\omega}, \quad (6)$$

or with substitution:

$$\frac{\alpha_{BR}}{h\omega} = \frac{n_K^0}{E} = D_2 N_K \quad (7)$$

$$\frac{\alpha_K}{h\omega} = D_{12} + D_2(1 - N_K) = \frac{N_K + n_K^0 - n_K - n_K^0 N_K}{EN_K}. \quad (8)$$

To improve the accuracy of the N_K determination, absorption spectra of BR-570 and K-590 are measured. Low energy (0.05 mJ/mm^2) dye laser pulses delayed 20 ns after 532-nm excitation are used to probe absorbance changes in the sample as a function of wavelength. These time-resolved absorbance measurements monitor the BR-570 and K-590 mixture, A_{BR+K} (Fig. 5). The absorbance of ground-state BR-570, A_{BR}, is measured directly from the sample without excitation (Fig. 5). The absorbance of K-590 alone can be calculated because:

$$A_K = A_{BR} + \frac{(A_{BR+K} - A_{BR})}{N_K}. \quad (9)$$

If it is assumed that both $\Phi_{BR\rightarrow K}$ and $\Phi_{K\rightarrow BR}$ are not functions of wavelength in the 620–700-nm region, then the spectral dependence in the A_K versus probe wavelength and the α_K versus excitation wavelength plots should quantitatively agree. Since these two plots depend on N_K differently, the N_K values used in expressions 6 and 7 can be varied to obtain the best agreement. Comparisons of spectral dependence are readily made in terms of α_K/A_K. The spectral shapes of the $A_K(\lambda)$ and $\alpha_K(\lambda)$ plots are found to be the same ($\pm 15\%$) for an $N_K = 0.36 \pm 0.02$. The resultant $\alpha(\lambda)$ and $A(\lambda)$ dependencies calculated using expressions 5–7 for BR-570 and K-590 are presented in Figs. 4 and 5, respectively.

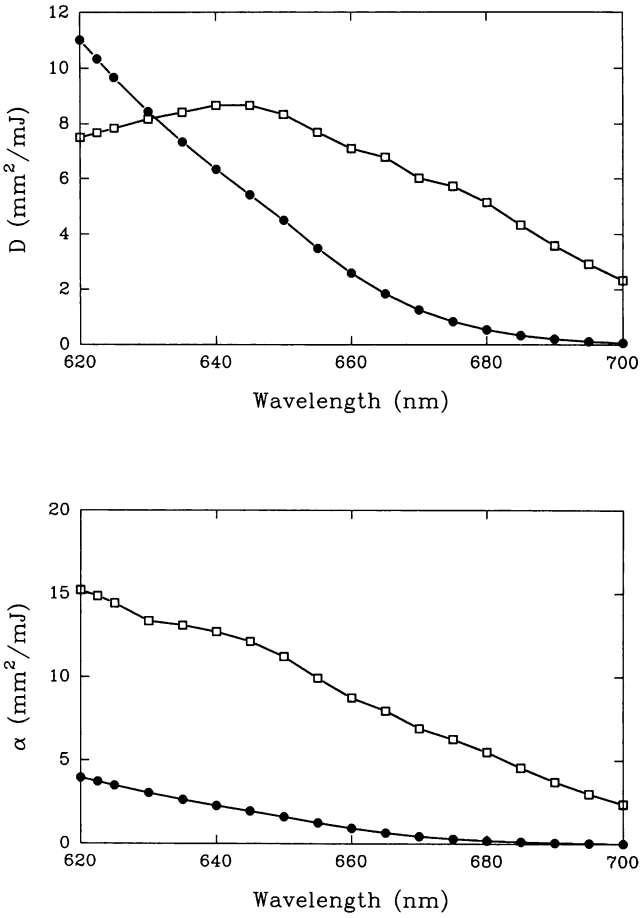

FIGURE 4 (*Top*) Normalized 633-nm probe laser absorbance (D represents both D_{12} and D_2, see text) changes measured for double-pulse excitation (532 nm followed at 20-ns delay by dye laser excitation; *open squares*) and for dye laser excitation only (*filled circles*). (*Bottom*) Calculated spectral dependence of the efficiencies for the BR → K (*filled circles*, α represents $(\alpha_{BR}/h\omega)$ and K → BR (*open squares*, α represents $(\alpha_K/h\omega)$ reactions using expressions 7 and 8.

With a photolytically-interrupted BR photocycle of $BR_{570} + h\nu \rightarrow BR^* \rightarrow J_{625} \rightarrow K_{590} + h\nu \rightarrow K^* \rightarrow BR_{570}$, the maximum achievable efficiency of K → BR with high

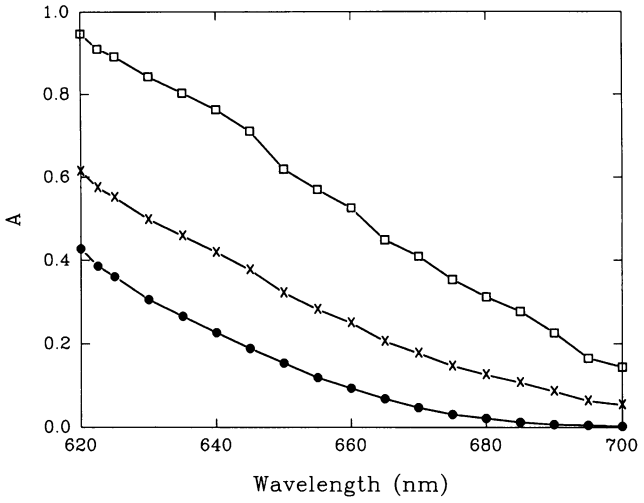

FIGURE 5 Absorption spectra measured for BR-570 (low power, probe dye laser beam only; *filled circles*) and for BR-570 together with K-590 (low power, probe dye laser appearing 20 ns after 532-nm excitation; *crosses*). Absorption spectrum calculated for K-590 alone from difference of [BR-570 + K-590] minus [BR-570 only] data (*open squares*). A represents A_{BR}, A_K, and A_{BR+K} (see expression 7 in text).

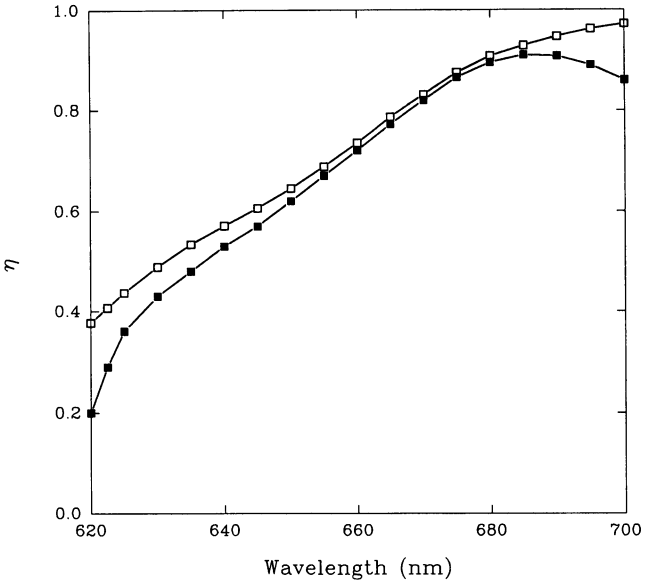

FIGURE 6 Spectral dependence of the percentage of K-590 optically converted back to BR-570 (η). The experimental data are shown as filled squares and the values calculated from the spectral dependence of the efficiency (expression 8) are shown as open squares.

energy, 10-ns excitation is given by:

$$\eta = \frac{(N_K - n_K)}{N_K} = 1 + \frac{\alpha_{BR}}{N_K(\alpha_{BR} + \alpha_K)}. \quad (10)$$

The spectral dependence based on this predicted η value can be compared with experimental measurements performed with the maximum energy density available in an unfocused beam from the dye laser operated near the center of the tuning curve (≈ 10 mJ/mm^2). The calculated and measured curves are close to one another in the center of the dye laser tuning range (Fig. 6), but differences appear at the edges of the tuning range where the dye laser energy is not high enough to produce the same photostationary mixture. The maximum efficiency for K → BR is obtained with a 685-nm excitation wavelength and an $\approx$8-mJ/mm^2 energy density ($\approx$95% of the K-590 formed by 532 nm excitation is returned to BR-570; Fig. 6). Larger K → BR conversion efficiencies may be achievable for dye laser wavelengths farther in the red, but significant laser energies beyond 700 nm are not available from the laser system used.

The data presented here make it feasible to calculate the relative efficiencies of BR → K and K → BR reactions from a comparison of α/A values. This ratio of efficiencies is equivalent to the ratio of quantum yields for the two reactions if sufficiently low energy 620–700-nm excitation is used,

$$\frac{\Phi_{K\rightarrow BR}}{\Phi_{BR\rightarrow K}} = \frac{\alpha_K \sigma_{BR}^{633nm}}{\alpha_{BR}\sigma_K^{633nm}} = \frac{\alpha_K A_{BR}}{\alpha_{BR} A_K}. \quad (11)$$

The ratio of quantum yields (Φ_{K-BR}/Φ_{BR-K}) is found to be 1.6 ± 0.1.

The quantum yield ratio provides some insight into the room temperature K → BR mechanism. With Φ_{BR-K} at room temperature being 0.64, as reported recently (15, 27), this ratio shows Φ_{K-BR} to be $\approx$ 1.0. The Φ_{BR-K} is measured for low energy excitation (15, 27), which corresponds to the low energy excitation conditions used here to determine the α/A ratio. A Φ_{K-BR} value $\approx$ 1.0 is consistent with 0.96 and 0.93 values reported recently (15, 28). It should be noted, however, that a variety of values for Φ_{BR-K} at room temperature have been reported (0.25–0.7) (15, 18, 19, 27–30). The value for Φ_{K-BR} of 0.7 at 77K has been reported (18, 19), but it is not obvious that this value is relevant to the room temperature measurements.

These data also provide information on whether the common excited state (CES) model is part of the molecular mechanism(s) describing BR → K and K → BR. Earlier studies of low (77 K) temperature BR samples alternatively included and excluded a CES for the BR → K and K → BR reactions based on whether the respective quantum yields reported added to unity or

not (19, 20). Although these results may not directly relate to the room temperature mechanisms considered here, they do emphasize the importance the absolute quantum yields have played in determining the molecular mechanisms in the BR photocycle. The role of a CES in the room temperature BR photocycle also has been questioned previously (3, 31).

The CES considered most widely is BR*, which forms J-625, and subsequently K-590, with a quantum yield of ≈ 0.64 (15, 27) and, therefore, BR′ with a quantum yield of ≈ 0.36 (Fig. 2). If BR* is a CES for BR → K and K → BR, it must be concluded that the yield of BR-570 (BR′) from K* can not exceed the quantum yield of BR-570 (BR′) from BR* (i.e., 0.36). This conclusion is correct at low excitation energies (such as used in the experiments described here), where the CES → BR-570 quantum yield determines the overall conversion efficiency of both the forward and reverse reactions (i.e., repetitive excitation at high excitation energies is absent). Thus, a Φ_{K-BR} of ≈ 1.0 is not consistent with a CES mechanism for the primary events in the room temperature BR photocycle.

Finally, there are two mechanistic issues involving BR → K and K → BR which require additional study. First, it is important to note that Φ_{K-BR} is measured here to be ≈ 1.0, only 20 ns after the photocycle begins while Φ_{BR-K}, to which it is compared (15, 27), is assigned to the initial processes occurring earlier (10 ps) in the photocycle. It remains to be demonstrated whether Φ_{K-BR} is constant over the initial 20-ns interval or whether it varies as a result of molecular changes that occur during the initial 20 ns of the photocycle. It is likely that the molecular coordinates along which the forward BR → K reaction proceeds are not the same as those for the reverse K → BR reaction. The differences could be in either the retinal chromophore or the protein or both. If differences in Φ_{K-BR} exist, the experiments analogous to those described here need to be performed on artificial BR pigments obtained by either systematically replacing the all-*trans* retinal of the native membrane with chemically- and/or isotopically-modified retinals or selectively altering the amino acid sequence of the protein via site-directed mutagenesis. Such molecular changes have already been shown to significantly alter photocycle properties while providing new insight into the molecular mechanisms involved (32–34). Second, the 10-ns excitation pulse used to initiate the photocycle will effectively populate both BR* and K* (Fig. 2) and, thereby, will access reactive channels other than BR → K and K → BR. The data in Fig. 3 suggest that additional reactions are unlikely to affect these results, but this point requires reexamination with shorter (ps) pulsed excitation in which the population of K* is minimized.

CONCLUDING REMARKS

Photolytic interruption of BR photocycle from K-590 is shown to proceed with efficiencies of >95% using nanosecond excitation of several mJ/mm^2 in the red (680–700 nm). Higher K → BR efficiencies may be found at longer excitation wavelengths, but it is clear that larger pulse energy densities lead to rapid sample degradation. The quantum yield of the K → BR reaction is found to be 1.6 ± 0.1 times larger than that of the BR → K reaction. When compared with the BR → K quantum yield of ≈ 0.64 (15, 27), this ratio indicates that the K → BR quantum yield is ≈ 1.0. These results are not consistent with a mechanistic model in which the BR → K and K → BR reactions share a CES. Transient absorption spectra of K-590 recorded in the 620–700-nm spectral region with a 20-ns delay are reported. Investigations using picosecond time resolution of photolytic interruptions in native and artificial BR photocycles are underway to more clearly characterize the K → BR reaction mechanism.

The authors wish to thank Dr. T. Brack for helpful discussions and a careful reading of this paper.

Received for publication 16 July 1991 and in final form 27 January 1992.

REFERENCES

1. Oesterhelt, D., and W. Stoeckenius. 1971. Rhodopsin-like protein from the membrane of *Halobacterium halobium*. *Nature New Biol.* 233:149–152.
2. Lozier, R. H., R. A. Bogomolni, and W. Stoeckenius. 1975. Bacteriorhodopsin: a light-driven proton pump in *Halobacterium halobium*. *Biophys. J.* 15:955–962.
3. Ottolenghi, M. 1982. Molecular aspects of the photocycles of rhodopsin and bacteriorhodopsin: a comparative overview. *Methods Enzymol.* 88:470–490.
4. Bazhenov, V. Yu., M. S. Soskin, V. B. Taranenko, and M. V. Vasnetsov. 1989. Biopolymers for real-time optical processing. *In* Optical Processing and Computing. H. Arsenault, editor. Academic Press, New York. 125–152.
5. Hampp, N., and C. Braeuchle. 1990. Bacteriorhodopsin and its functional variants: potential applications in modern optics. *In* Photochromism: Molecules and Systems. H. Dürr and H. Bouas-Laurent, editors. Elsevier Science Publishers, Amsterdam-New York. 954–968.
6. Ippen, E. P., C. V. Shank, A. Lewis, and M. A. Marcus. 1978. Subpicosecond spectroscopy of bacteriorhodopsin. *Science (Wash. DC)*. 200:1279–1281.
7. Chernavskii, D. S., I. V. Chizhov, R. H. Lozier, T. M. Murina, A. M. Prokhorov, and B. V. Zubov. 1989. Kinetic model of bacteriorhodopsin photocycle: pathway from M state to bR. *Photochem. Photobiol.* 49:649–653.

8. Shichida, Y., S. Matuoka, Y. Hidaka, and T. Yoshizawa. 1983. Absorption spectra of intermediates of bacteriorhodopsin measured by laser photolyses at room temperature. *Biochem. Biophys. Acta.* 723:240–246.
9. Stern, D., and R. Mathis. 1985. Picosecond and nanosecond resonance Raman evidence for structural relaxation in bacteriorhodopsin's primary photoproduct. *In* Time Resolved Vibrational Spectroscopy. A. Lauberaeu and M. Stockburger, editors. Springer-Verlag, New York. 250–254.
10. Milder, S. J., and D. S. Kliger. 1988. A time-resolved spectral study of the K and KL intermediates of bacteriorhodopsin. *Biophys. J.* 53:465–468.
11. Diller, R., and M. Stockburger. 1988. Kinetic resonance Raman studies reveal different conformational states of bacteriorhodopsin. *Biochemistry.* 27:7641–7651.
12. Hanamoto, J. H., P. Dupuis, and M. A. El-Sayed. 1984. On the protein (tyrosine)-chromophore (protonated Schiff base) coupling in bacteriorhodopsin. *Proc. Natl. Acad. Sci. USA.* 81:7083–7087.
13. Birge, R. R., T. M. Cooper, A. F. Lawrence, M. B. Masthay, C.-F. Zang, and R. Zidovetzki. 1991. Revised assignment of energy storage in the primary photochemical event in bacteriorhodopsin. *J. Am. Chem. Soc.* 113:4327–4328.
14. Goldschmidt, C. R., M. Ottolenghi, and R. Korenstein. 1976. The primary quantum yields in the bacteriorhodopsin photocycle. *Biophys. J.* 16:839–843.
15. Govindjee, S. P. Balashov, and T. G. Ebrey. 1990. Quantum efficiency of the photochemical cycle of bacteriorhodopsin. *Biophys. J.* 58:597–608.
16. Sasaki, N., F. Tokunaga, and T. Yosizawa. 1983. Two forms of intermediates of frog rhodopsin in rod outer segments. *Biochim. Biophys. Acta.* 722:80–87.
17. Stoeckenius, W., and R. H. Lozier. 1974. Light-energy conversion in *Halobacterium halobium. J. Supramol. Struct.* 2:769–773.
18. Goldschmidt, C. R., O. Kalisky, T. Rosenfeld, and M. Ottolenghi. 1977. The quantum efficiency of bacteriorhodopsin photocycle. *Biophys. J.* 17:179–183.
19. Becher, B., and T. G. Ebrey. 1977. The quantum efficiency for the photochemical conversion of the purple membrane protein. *Biophys. J.* 17:185–191.
20. Kryukov, P. G., Yu. A. Matveets, A. V. Sharkov, Yu. A. Lasarev, and E. L. Terpugov. 1980. Direct and reverse photoreactions in bacteriorhodopsin in low temperatures on picosecond time scales. *Springer Ser. Opt. Sci.* 22 (*Lasers Photomed. Photobiol.*): 200–206.
21. Kryukov. P. G., Yu. A. Lasarev, Yu. A. Matveets, E. L. Terpugov, L. N. Chekulaeva, and A. V. Sharkov. 1981. Picosecond spectroscopy of deuterated acteriorhodopsin on the primary picosecond event. *Stud. Biophys.* 83:101–108.
22. Iwasa, T., Y. Suzuki, T. Nakayama, F. Tokunaga, and M. Hirai. 1984. Picosecond spectroscopy on reverse photoreaction from batho-intermediate of bacteriorhodopsin at 6.5 K. *J. Physiol. Soc. Jpn.* 53:2851–2856.
23. Grieger, I., and G. H. Atkinson. 1985. Photolytic interruption of the bacteriorhodopsin photocycle examined by time-resolved resonance Raman scattering. *Biochemistry.* 24:5660–5665.
24. Kaufmann, K. J., P. M. Rentzepis, W. Stoeckenius, and A. Lewis. 1976. Primary photochemical processes in bacteriorhodopsin. *Biochem. Biophys. Res. Commun.* 68:1109–1115.
25. Applebury, M. L., K. S. Peters, and P. M. Rentzepis. 1978. Primary intermediates in the photochemical cycle of bacteriorhodopsin. *Biophys. J.* 23:375–382.
26. Oesterhelt, D., and W. Stoeckenius. 1974. Isolation of the cell membrane of *Halobacterium Halobium* and its fractionation into red and purple membrane. *Methods Enzymol.* 31:667–671.
27. Tittor, J., and D. Oesterhelt. 1990. The quantum yield of bacteriorhodopsin. *FEBS Letts.* 263:269–273.
28. Dioumaev, A. K., V. V. Savransky, N. V. Tkachenko, and V. I. Chukhraev. 1989. Quantum yield and extinction measurements in strongly overlapping reactant and photoproduct absorption bands. II. Bathointermediate formation in bacteriorhodopsin photocycle at room temperature. *J. Photochem. Photobiol. B.* 3:397–410.
29. Hurley, J., and T. Ebrey. 1977. The quantum efficiency for the photochemical conversion of the purple membrane protein. *Biophys. J.* 17:185–191.
30. Schneider, G., R. Diller, and M. Stockburger. 1989. Photochemical quantum yield of bacteriorhodopsin from resonance Raman scattering as a probe for photolysis. *Chem. Phys.* 131:17–29.
31. Ottolenghi, M., and M. Sheves. 1987. On the nature of the primary photochemical events in rhodopsin and bacteriorhodopsin. *In* Primary Processes in Photobiology, Springer Proceedings in Physics 20. T. Kobayashi, editor. Springer Verlag, New York. 144–153.
32. Ottolenghi, M., and M. Sheves. 1989. Synthetic retinals as probes for the binding sites and photoreactions in rhodopsins. *J. Membr. Biol.* 112:193–212.
33. Hampp, N., C. Brauchle, and D. Oesterhelt. 1990. Bacteriorhodopsin wild-type and variant aspartate-96 → asparagine as reversible holographic media. *Biophys. J.* 58:83–93.
34. Sakmar, T., R. R. Franke, and H. G. Khorana. 1989. Glutamic acid-113 serves as the retinylidene in Schiff base counterion in bovine rhodopsin. *Proc. Natl. Acad. Sci. USA.* 86:8309–8313.